

## Semiconstant-Time ${}^{31}\text{P}$ , ${}^1\text{H}$ -COSY NMR: Analysis of Complex Mixtures of Phospholipids Originating from *Helicobacter pylori*

Katja Petzold,<sup>†</sup> Annelie Olofsson,<sup>†</sup> Anna Arnqvist,<sup>†</sup> Gerhard Gröbner,<sup>‡</sup> and Jürgen Schleucher<sup>\*†</sup>

Medical Biochemistry and Biophysics, Department of Chemistry, Umeå University,  
KBC Building, S-90187 Umeå, Sweden

Received June 26, 2009; E-mail: jurgen.schleucher@chem.umu.se

Virtually every process in living organisms proceeds via biological membranes and their constituents.<sup>1</sup> These membranes have a unique evolutionary structural and functional organization, which enables them to simultaneously act as a cellular compartmentalization barrier, to control communication between the cell and its surroundings, and to perform vital metabolic processes. In general, membranes consist of proteins and lipids, where the latter not only provide the basic membrane scaffold but also are often required in specific composition for many membrane proteins to function. Unfortunately, through evolution pathogens have also refined their membrane-associated systems to communicate with and infect their host organism.<sup>2</sup> One of the most widespread pathogens is *Helicobacter pylori* (*H. pylori*), which survives in the acidic stomach environment. It infects the stomachs of more than 50% of the population worldwide and causes a lifelong infection if not treated. Of the infected individuals, 10% develop symptoms such as peptic ulcer and 1% develop gastric cancer.<sup>3</sup> An important prerequisite for achieving persistent infection is bacterial adherence to the stomach mucosa. Specific adherence proteins, so-called adhesins, are incorporated in the outer membrane, displayed on the bacterial surface, and mediate tight adherence to the host epithelial surface.<sup>3,4</sup> As background to understand the adhesin-mediated virulence of *H. pylori*, we here analyze the membrane lipid environment of the proteins, which presumably tightly controls their function.

Routine methods of analysis of the phospholipid composition of membranes include thin layer chromatography, mass spectrometry, high-pressure liquid chromatography, and nuclear magnetic resonance (NMR).<sup>5,6</sup> Potentially, the NMR approach has several advantages. It can analyze simultaneously each component in a complex lipid mixture, thereby avoiding time-consuming and error-prone separation of lipids, it can avoid the use of numerous external lipid reference standards, and it can easily yield structural information for as yet unknown lipids. Finally, the lipid sample can be recovered effortlessly after the NMR experiments. The  ${}^{31}\text{P}$  nucleus plays a unique role in phospholipid analysis because it senses the headgroup and glycerol moiety simultaneously.  ${}^{31}\text{P}$  has 100% abundance and good relaxation properties, but the small chemical shift dispersion and the dependence of the chemical shift on the solvent composition can seriously interfere with the unambiguous identification of phospholipids.<sup>5</sup> Here, we present a novel semiconstant-time 2D  ${}^{31}\text{P}$ , ${}^1\text{H}$  COSY experiment that allows reliable identification and quantification of phospholipids in complex mixtures, based on  ${}^{31}\text{P}$  and  ${}^1\text{H}$  chemical shifts and  $J$ -couplings.

The pulse sequence of the semiconstant-time 2D  ${}^{31}\text{P}$ , ${}^1\text{H}$ -COSY is presented in Figure 1. After excitation of the  ${}^{31}\text{P}$  nuclei,  ${}^{31}\text{P}$ , ${}^1\text{H}$   $J$ -couplings and  ${}^{31}\text{P}$  chemical shift evolve in a semiconstant-time<sup>7</sup> manner for  $2\Delta = 20$  ms and  $t_{1,\text{max}} = 60$  ms, respectively. These

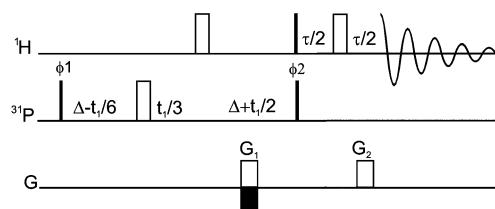


**Figure 1.** Pulse sequence of the semiconstant-time  ${}^{31}\text{P}$ , ${}^1\text{H}$ -COSY. Narrow and wide bars indicate nonselective  $90^\circ$  and  $180^\circ$  pulses with phase  $x$  unless specified otherwise.  ${}^{31}\text{P}$ , ${}^1\text{H}$  couplings and  ${}^{31}\text{P}$  chemical shift develop simultaneously as semiconstant time evolution. Gradients  $G_1$ ,  $G_2$  were of 900, 300  $\mu\text{s}$  duration and 30, 36.5 G/cm amplitude, respectively, followed by a 300  $\mu\text{s}$  delay. The gradient ratio is fine-tuned to generate a heteronuclear gradient echo, which creates clean spectra.  $G_1$  is inverted in alternate FIDs for echo-antiecho sign discrimination in  $t_1$ .<sup>10</sup> Phase cycling:  $\phi_1$ :  $x, -x$ ;  $\phi_2$ :  $2x, 2-x$ ; rec:  $x, 2-x, x$ .

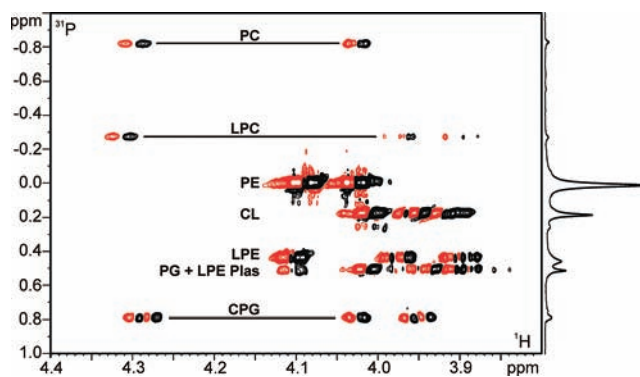


**Figure 2.** 2D semiconstant-time  ${}^{31}\text{P}$ , ${}^1\text{H}$ -COSY spectrum of phospholipids from *H. pylori* cells,<sup>11</sup> recorded at 298 K on a Bruker DRX600 spectrometer equipped with an HCP cryo-probe. Negative contours are colored red, and for comparison a direct-detect  ${}^{31}\text{P}$  spectrum is presented to the right. Each coupled  ${}^{31}\text{P}$ , ${}^1\text{H}$  pair of the headgroup or glycerol moiety creates an antiphase cross-peak. See text for abbreviations.

parameters minimize relaxation losses during  $2\Delta$  and yield high-resolution singlet signals in the  ${}^{31}\text{P}$  dimension (Figure 2). Furthermore,  ${}^{31}\text{P}$ , ${}^1\text{H}$  coupling evolution, which prepares for coherence transfer to  ${}^1\text{H}$  for detection, has a similar efficiency for all phospholipids, which is essential for quantification. After coherence transfer,  ${}^1\text{H}$  signals are detected, which is inherently more sensitive than  ${}^{31}\text{P}$  detection, and the increase can be amplified by using a cryo-probe. A heteronuclear gradient echo suppresses all signals lacking  ${}^{31}\text{P}$ , ${}^1\text{H}$  couplings. The signals detected show  $J_{\text{HP}}$  couplings in antiphase and  $J_{\text{HH}}$  couplings in-phase. The resulting coupling patterns allow reliable identification of phospholipids (Figures 2, 3). Other 2D  ${}^1\text{H}$ , ${}^{31}\text{P}$  correlation experiments (HMBC,<sup>8</sup> P-HSQC-TOCSY<sup>9</sup>) either do not give pure phases, which degrades resolution, or lose the coupling patterns used to identify lipids. A mixture of common lipids was used to estimate the sensitivity of the experi-

<sup>†</sup> Medical Biochemistry and Biophysics.

<sup>‡</sup> Department of Chemistry.

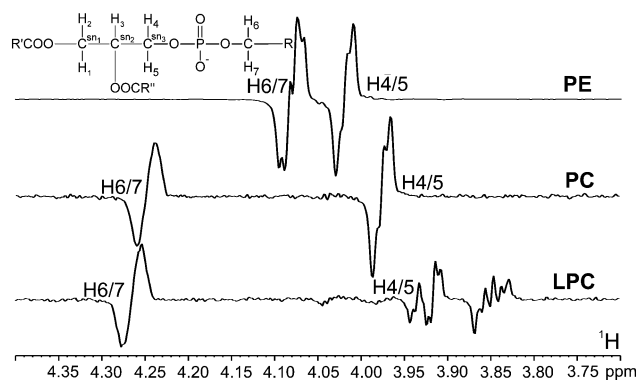


**Figure 3.**  $^1\text{H}$  traces extracted from the 2D NMR spectrum shown in Figure 2. Multiplet structures are due to  $J_{\text{HP}}$  (antiphase) and  $J_{\text{HH}}$  (in-phase). The insert shows a general phospholipid structure and the assignment of protons coupled to phosphorus. Coupling patterns of head groups (H6/7) and the glycerol moiety (H4/5) are characteristic of the structures of each moiety.

ment. The detection limit for individual phospholipids was  $\sim 3 \mu\text{g}$  ( $10 \mu\text{M}$ ) in an overnight experiment (600 MHz spectrometer with cryo-probe; see Supporting Information for experimental parameters).

To analyze *H. pylori* membrane lipid composition, we extracted lipids from whole cells.<sup>11</sup> Phospholipid identification in the 2D spectra (Figure 2) was based on  $^1\text{H}$  and  $^{31}\text{P}$  chemical shifts<sup>12</sup> and the patterns created by  $^3J_{\text{HP}}$  and  $J_{\text{HH}}$  couplings. Main components were phosphatidylethanolamine (PE), cardiolipin (CL), *sn*-2 lysophosphatidylethanolamine (LPE), and phosphatidylglycerol (PG). Phosphatidylcholine (PC), *sn*-2 lysophosphatidylcholine (LPC), *sn*-2 lyso-phosphatidylethanolamine plasmalogen (LPE Plas),<sup>13</sup> and a cholesteryl phosphoglucoside derivative (CPG) were identified as minor components. Note that only the 2D spectrum reveals that, at 0.5 ppm  $^{31}\text{P}$  chemical shift, the signals of PG and LPE Plas are completely overlapped in the direct-detect  $^{31}\text{P}$  spectrum (Figure 2). All identified lysophospholipids (LPLs) lack the *sn*-2 chain, based on the drastically changed coupling pattern of the glycerol moiety (H4/5 in Figure 3). These changes are caused by formation of a hydrogen bond between the C2–OH of glycerol and the phosphate group.<sup>14</sup> Thus, the new NMR approach provides an unambiguous identification of LPLs irrespective of changes in chemical shift.

Quantification of phospholipids is readily achieved by picking peak heights of individual cross-peaks in the 2D spectra. This even allows quantification of phospholipids with completely overlapping  $^{31}\text{P}$  signals, such as PG and LPE Plas in Figure 2, as long as one  $^{31}\text{P}$ ,  $^1\text{H}$  cross-peak of each lipid is resolved. In general, variation in coupling constants among phospholipids can lead to different coherence transfer efficiencies. Therefore parameters of our experiment were optimized to minimize these differences, resulting in

similar and well reproducible transfer factors for all lipids (Table S1). Thus, variation in phospholipid composition can easily be detected with the new experiment, and absolute quantification of lipid composition is possible. The *H. pylori* lipid extract used here contained 13% LPE and 1% LPC. While high amounts of LPLs have been reported previously,<sup>15</sup> the new experiment allows studying the role of these unusual amounts of LPLs for the functions of different *H. pylori* membrane systems during different stages of infection.<sup>11</sup>

The new semiconstant-time  $^{31}\text{P}$ ,  $^1\text{H}$ -COSY sequence, presented here, is a highly sensitive approach for identification and precise quantification not only of phospholipids but also of other organic phosphorus compounds in research fields ranging from signal transduction to phosphorus cycling in soils.<sup>16</sup>

**Acknowledgment.** We thank Anna Vallström, Leif Rilfors, and Carina Lundberg for discussions. This work was supported by UCMR, the Kempe and Wallenberg Foundations (K.P., J.S.), the Swedish Research Councils VR and formas (G.G., A.A., J.S.), Cancerfonden (A.A.), and “Insamlingstiftelse” of Umeå University (J.S., G.G.).

**Supporting Information Available:** Listing of pulse sequence, description of experimental protocol, table with transfer factors, complete list of authors for ref 2. This material is available free of charge via the Internet at <http://pubs.acs.org>.

## References

- (1) Yeagle, P. *The Structure of Biological Membranes*; CRC: 2004; p 552.
- (2) Linz, B.; et al. *Nature* **2007**, *445*, 915–918.
- (3) Cover, T.; Berg, D. E.; Blaser, M. J.; Mobley, H. H. *Y. pylori Pathogenesis*; Groisman, E. A., Ed.; Academic: New York, 2001; pp 509–558.
- (4) Yamaoka, Y.; Alm, R. A. *Helicobacter Pylori Outer Membrane Proteins*; Yamaoka, Y., ed.; Horizon Scientific Press: 2008; pp 37–61.
- (5) Schiller, J.; Arnold, K. *Med. Sci. Monit.* **2002**, *8*, MT205–222.
- (6) Lindblom, G.; Gröbner, G. *Curr. Opin. Colloid Interface Sci.* **2006**, *11*, 24–29.
- (7) Grzesiek, S.; Bax, A. *J. Biomol. NMR* **1993**, *3*, 185–204. Logan, T. M.; Olejniczak, E. T.; Xu, R. X.; Fesik, S. W. *J. Biomol. NMR* **1993**, *3*, 225–231.
- (8) Bax, A.; Griffey, R. H.; Hawkins, B. L. *J. Magn. Reson.* **1983**, *55*, 301–315.
- (9) Henke, J.; Willker, W.; Engelmann, J.; Leibfritz, D. *Anticancer Res.* **1996**, *16*, 1417–1427.
- (10) Sattler, M.; Schleucher, J.; Griesinger, C. *Prog. Nucl. Magn. Reson. Spectrosc.* **1999**, *34*, 93–158.
- (11) Olofsson, A.; Vallström, A.; Petzold, K.; Schleucher, J.; Carlsson, S.; Nyunt Wai, S.; Gröbner, G.; Arnqvist, A., submitted.
- (12) Meneses, P.; Glonek, T. *J. Lipid Res.* **1988**, *29*, 679–689. Metz, K. R.; Dunphy, L. K. *J. Lipid Res.* **1996**, *37*, 2251–2265. Sparling, M. L.; Zidovetzki, R.; Muller, L.; Chan, S. I. *Anal. Biochem.* **1989**, *178*, 67–76. Wang, Y.; Hollingsworth, R. I. *Anal. Biochem.* **1995**, *225*, 242–251.
- (13) Sacchi, R.; Medina, I.; Paolillo, L. *Chem. Phys. Lipids* **1995**, *76*, 201–209.
- (14) Pascher, I.; Sundell, S.; Hauser, H. *J. Mol. Biol.* **1981**, *153*, 807–824.
- (15) Tannaes, T.; Bukholm, I. K.; Bukholm, G. *FEMS Immunol. Med. Microbiol.* **2005**, *44*, 17–23.
- (16) Cade-Menun, B. J. *Talanta* **2005**, *66*, 359–371.

JA905282H